Processing of Poly(Amide Imides) as Matrices for High-Performance Composites

S. DOUGLAS COPELAND,[1] JAMES C. SEFERIS,*[,1] and MARC CARREGA[2]

[1]Polymeric Composites Laboratory, Department of Chemical Engineering, University of Washington, Seattle, Washington 98195 and [2]Rhone-Poulenc Chimie, 92097 Paris-La Defense, France

SYNOPSIS

Poly(amide imide) (PAI) has proven to be an excellent engineering thermoplastic. Injection and compression molding processes are currently used to produce poly(amide imide) parts when superior toughness, solvent resistance, and high-temperature heat performance are required. The objective of this work was to determine the essential features necessary to use these systems as matrices for carbon-fiber-reinforced composites. The principal steps utilized were: impregnation of the carbon fibers with a PAI solution, drying the solvent from the individual plies, stacking the plies for final consolidation, and a postcure. A processing cycle was developed applicable to resins with different solvent concentration and molecular weight, giving special attention to the solvent evaporation step. A model capable of predicting the rate of evaporation as a function of temperature was developed using the principle of time–temperature superposition. A viscosity model similar to that for a curing thermoset was developed by combining Arrhenius expressions for the temperature and concentration effects. Collectively, this work then provided insight for matrix requirements in the formulation of PAI composites by solvent impregnation.

INTRODUCTION

Amorphous thermoplastics are often preferred over semicrystalline ones because their mechanical properties are virtually independent of the processing conditions. Amorphous polymers are being studied for use in metallic glasses, as well as for amorphous semiconductors.[1] Although the poly(amide imides) may be considered amorphous systems, they are not true thermoplastics. Poly(amide imides) can be processed using established injection molding and extrusion techniques typical of thermoplastics, but they actually undergo a crosslinking reaction at elevated temperatures.[2] This crosslinking gives a higher glass transition temperature and better creep and solvent resistance to a polymer that already has excellent mechanical properties.[3,4]

Poly(amide imide) (PAI) has been available for more than 15 years, with structural applications in automotive, aerospace, and electronic industries. PAI has reportedly the highest strength of any commercial unreinforced plastic, with a tensile strength in excess of 172 MPa (25,000 psi), and a heat distortion temperature of 275°C (525°F) with a load of 1.82 MPa (264 psi).[5] It also has excellent toughness and thermal properties.[6] Poly(amide imides) have also been produced as adhesives, fibers, and for fire-resistant applications for more than 15 years. These properties make PAIs strong candidates as matrices for high-performance composites. However, very little work has been done because of difficult processing requirements. Their high viscosities require the use of organic solvents such as *N*-methyl pyrrolidone and dimethylformamide for impregnation of the fibers. The use of solvents may give some difficulty with environmental/health issues, while creation of voids in the composite must also be considered.[7] Fortunately, the chemistry of a PAI is such that the molecular weight of the intermediate polymer at the prepreg stage can be controlled to improve

* To whom correspondence should be addressed.

Journal of Applied Polymer Science, Vol. 44, 41–53 (1992)
 CCC 0021-8995/92/010044-13$04.00

processability without decreasing the ultimate molecular weight.[8]

With all the problems associated with PAIs, they still offer potential for high-temperature performance and flammability. In this investigation, we evaluated the potential of using existing PAIs, currently in use as adhesives and fibrous solutions, as matrices for high-performance composites. The basic goal of this work was to identify a window of required processing conditions and desired polymer physical properties for the manufacture of PAI matrix composites.

EXPERIMENTAL

Materials

Three different commercially available PAI resins were supplied by Rhone-Poulenc. The system chemistry is schematically illustrated in Figure 1. The systems differed in molecular weight and viscosity and were available as solutions in the solvent, *N*-methyl pyrrolidone (NMP). Pertinent data are summarized in Table I.

Thermal analysis was used to characterize the different resins. Specifically, thermogravimetric analysis (TGA), differential scanning calorimetry (DSC), and dynamic mechanical analysis (DMA) experiments were performed using a DuPont thermal analysis system.

The viscosity of the three solutions was measured using a Wells-Brookfield cone and plate microviscometer. Viscosity, as a function of temperature, was

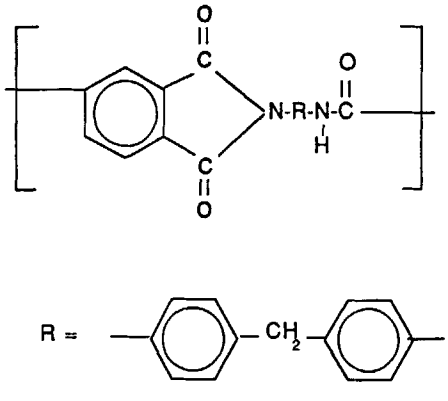

Figure 1 Schematic representation of the poly(amide imide) repeat unit showing imide and amide linkages. The backbone may be modified with different substitution of R.

Table I Poly(amide imide) Resins

Resin	Number Average Molecular Weight	Percent Polymer in NMP Solution
A	8,600	27
B	16,500	27
C	24,600	22

measured by circulating heated oil through the plate of the instrument. Polymer C was available both in solution and powder form. The viscosity of the powder was measured at 0.308, 0.278, 0.250, and 0.235 weight fraction polymer in NMP solution from 25 to 60°C. TGA experiments were performed at the same heating rate used in the viscometer to produce time, temperature, and concentration data.

The resin uptake of carbon fiber tows was measured by submersing the tows in the resin for 3 h and then scraping off the excess from the surface. The wetting characteristics of the PAI solution were examined using optical microscopy with a Nikon polarizing microscope. Impregnation of unidirectional fibers was performed using a small-scale hot melt prepregger.[9] In addition, unidirectional carbon fiber tows, held together by a polymer strip and plain weave cloth, were impregnated by manually spreading the solution into the fiber bed. The prepreg was dried in a circulating oven.

The prepreg was stacked and wrapped with semipermeable bleeder cloth to prevent spreading of the unidirectional fibers. Semipermeable bleeder cloth was used to allow evaporation of the solvent. The laminates were processed both in a hydraulic press (Tetrahedron) and in an autoclave (Lipton Steel). Finally, optical microscopy was used to evaluate void content in the laminates.

Differential scanning calorimetry was performed using aluminum sample pans without lids to allow evaporation of the solvent. Although the DSC signal was noisy, pans without lids gave better results than if the samples were run with lids. The DSC scans of as-received solutions A, B, and C were quite similar.

Dynamic mechanical analysis of dried prepreg was performed for each solution. Carbon fiber cloth was impregnated with each resin, and the solvent was evaporated in the oven for 15 min at 150°C until the cloth was essentially dry. Four single plies were cut for DMA measurements from each cloth. The four plies were bound together and the samples were heated at 5°C/min from 50 to 400°C.

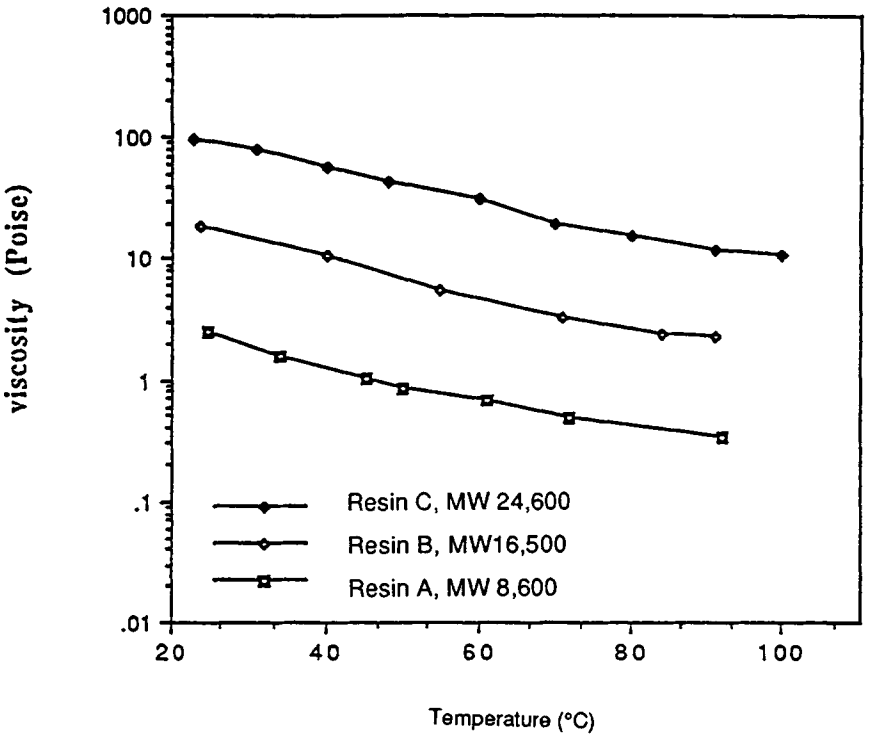

Figure 2 Viscosity of solutions of poly(amide imides) and NMP as a function of temperature.

RESULTS AND DISCUSSION

Characterization

The viscosities as a function of temperature for the three solutions examined in this work are shown in Figure 2. An increase in viscosity was observed with increasing molecular weight for the different solutions for all temperatures examined. The viscosity could be measured up to a temperature of approximately 100°C where the viscosity began to rise again. At that temperature, a film was observed to form on the bottom plate of the viscometer, which could be attributed to solvent evaporation.

TGA thermograms for each polymer solution were determined by two techniques. In the first technique, the polymer solution was measured as-received, which was 73% NMP solvent for solutions A and B, and 78% for solution C. The weight loss curves were dominated by evaporation of the solvent. As a result, in the second technique, the excess solvent was evaporated to obtain a thin flexible film. This enabled a better analysis for resin degradation. The scan showed two distinct weight loss regions. The NMP evaporated over a wide range of temperatures, while a sharp degradation peak was observed at 500°C, as can be seen in Figure 3.

The initial DSC scan of each polymer solution was dominated by the evaporation of NMP. DSC of the resins, following a 12-h postcure at 275°C, showed glass transition temperatures all in the range of 275°C, as can be seen in Figure 4. Dezern reported a clear exothermic recrystallization peak at 525°C, and an obvious melting endotherm at 575°C in a poly(amide imide) polymer.[10] In an attempt to duplicate these findings with solution C, a scan was performed up to 600°C. Although several peaks were observed, they could not be clearly identified as recrystallization and melting peaks. They were interpreted as peaks associated with the degradation of the polymer. The scan exhibited solvent evaporation at 100–200°C, crosslinking reaction at 300–350°C, and the onset of degradation at slightly higher temperatures.

The first and second DMA runs for four plies of carbon-fiber-reinforced resin B prepreg are shown in Figure 5. The DMA was run at the same heating rate as the previous TGA experiments to observe changes in stiffness as a result of evaporation of the solvent.

It was difficult to interpret the differences in the initial scans for each solution. Solution A showed much more dramatic changes in stiffness than either

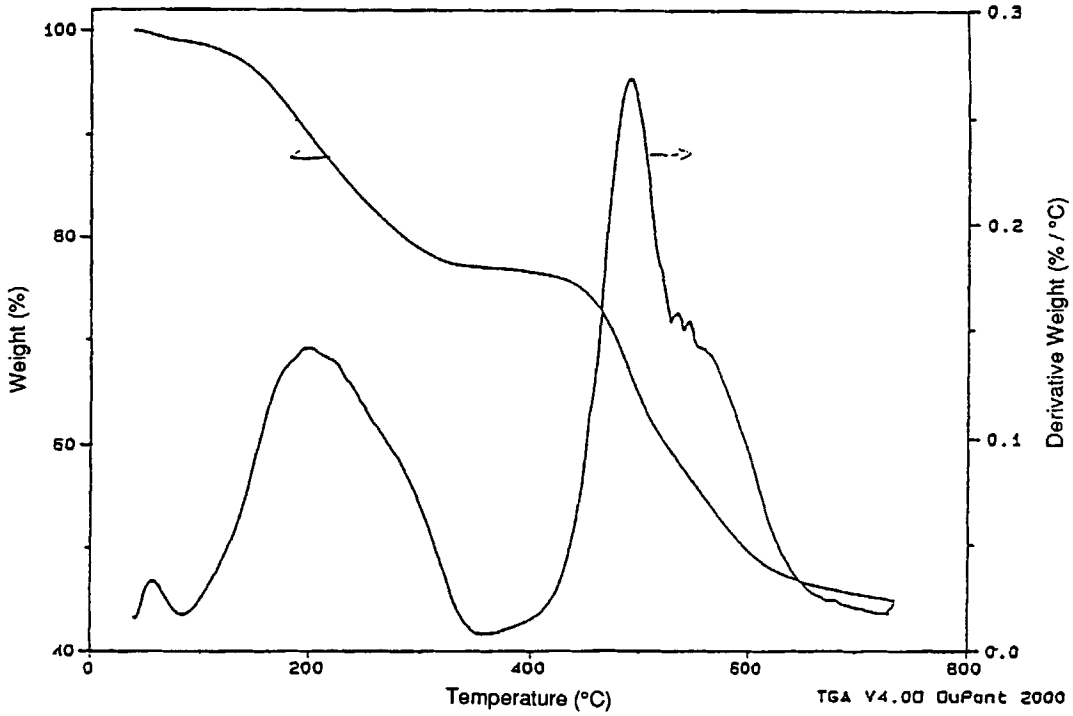

Figure 3 Thermogravimetric analysis (TGA) of sample C (M_w 24,600, 22% solvent). Heating rate was 5°C/min.

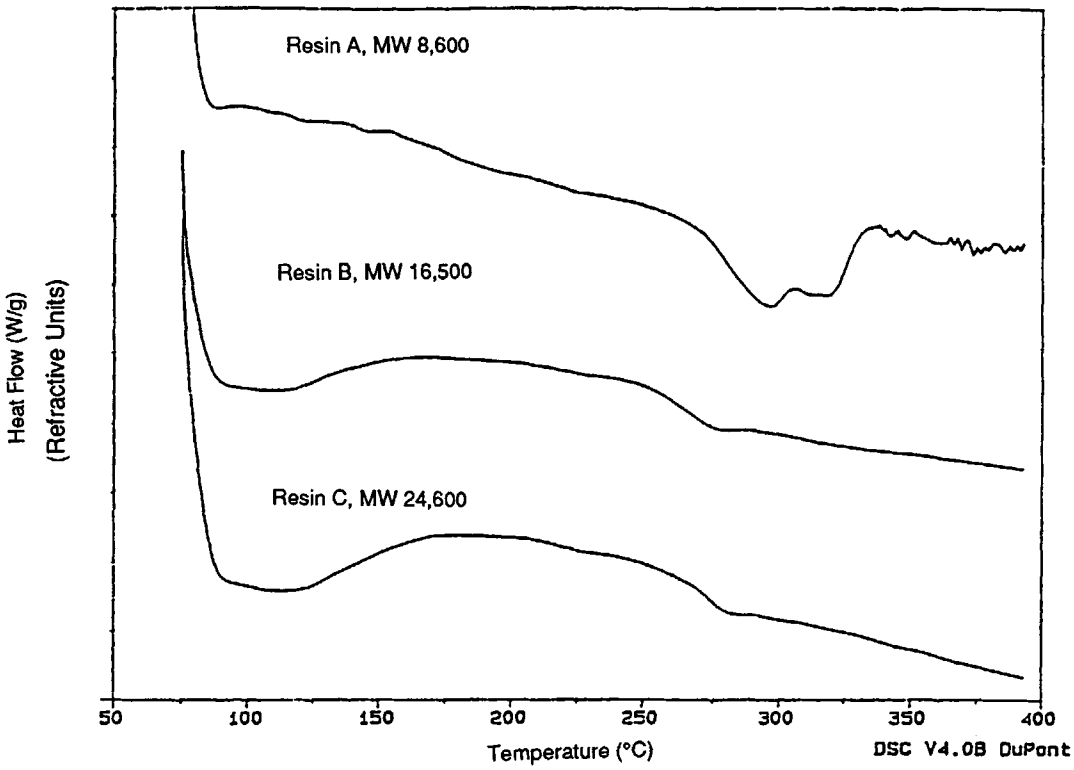

Figure 4 Differential scanning calorimetry (DSC) of the three resin systems after devolatilization and a postcure at 275°C. Heating rate was 5°C/min. Thermograms were shifted vertically for clarity.

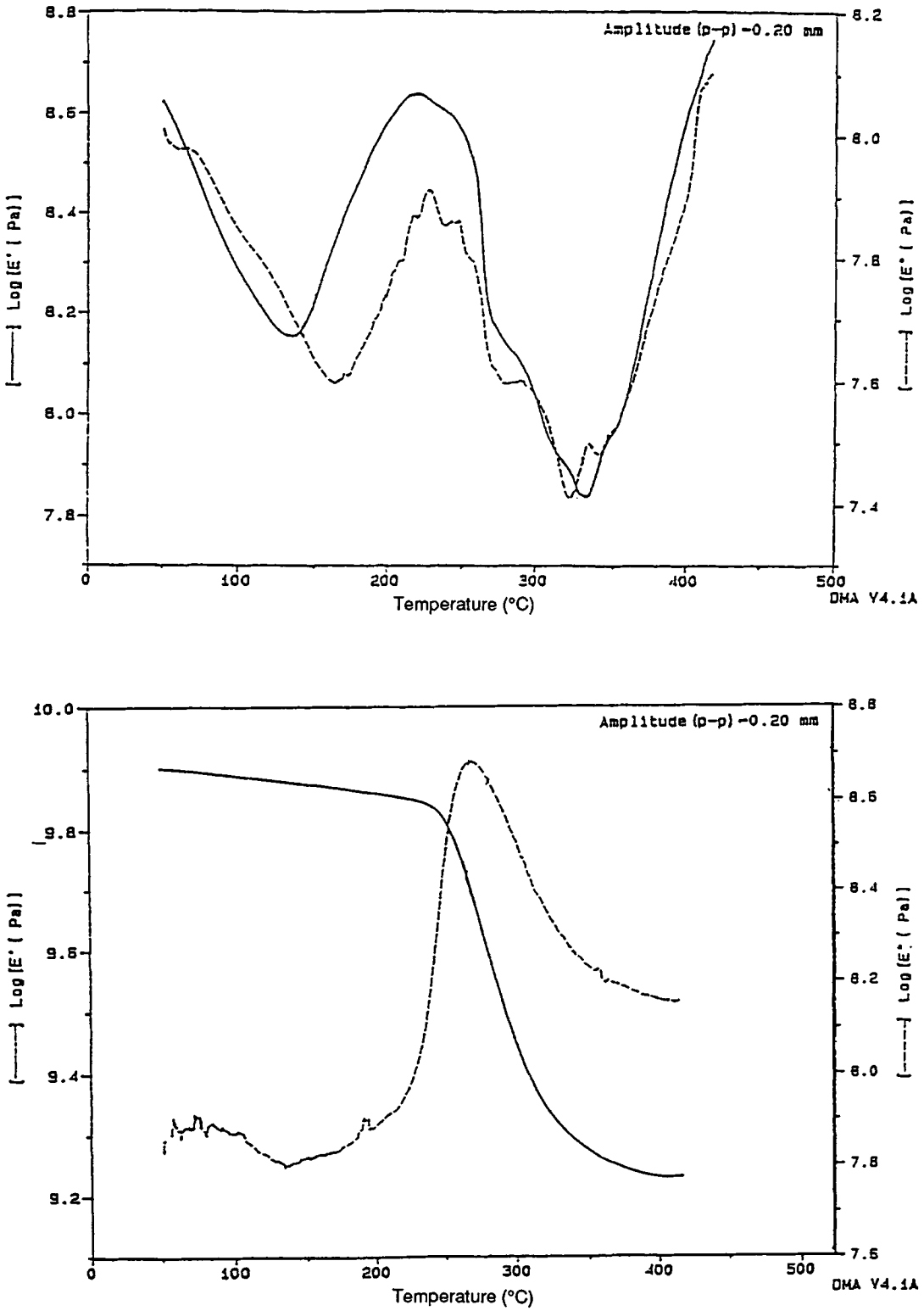

Figure 5 Dynamic mechanical analysis (DMA) for four plies of carbon-fiber-reinforced resin B (M_w 16,500) prepreg. Initial thermogram is shown at the top while the second thermogram is shown at the bottom.

Table II Resin Absorption by Carbon Fibers

Matrix Resin	Fiber Weight (g)	Total Weight (g)	Wt % Resin[a]
A	1.2061	6.2491	53
B	1.2629	6.4085	52
C	1.2877	5.7556	43

[a] Weight percent resin calculated assuming 100% of the solvent will be removed.

B or C. However, they all exhibited a decrease in stiffness as the temperature increased and the solvent evaporated. Once the majority of the solvent had evaporated, the modulus began to rise. The modulus reached a maximum at approximately 250°C before it began to drop again upon further heating. Each solution showed another increase in modulus slightly above 300°C. This increase was interpreted as the onset of the crosslinking reaction.

The samples were run again after they cooled down, and the clamps were retightened. Subsequent scans on the same samples gave modulus curves typical of cured composites. Samples A, B, and C had glass transition temperatures of 291.0, 304.7, and 330.8°C, identified by the exhibited maximum of the tan δ curve.

The wetting characteristics of the carbon fibers with the PAI resins were observed by soaking a bundle of fibers in the resin for 12 h and visually examining them. Optical microscopy showed the resin beading up on the individual fibers. A resin with good wetting characteristics will form a smooth, continuous layer along the surface of the fiber. Resin absorption by the fiber tows was measured by soaking the tows in the resin for 3 h. The initial weight of the fibers was recorded, and the final weight was measured after scraping as much excess resin as could be removed from the tows. The excess resin was scraped off to simulate what would be forced out of the composite when pressure is applied. The results are summarized in Table II.

Impregnation

Impregnation of carbon fibers with sample B was performed on a small-scale prepregging machine.[9] The concept of a prepreg flow number, developed by Ahn and Seferis, is helpful in understanding the prepregging process.[11] It is represented by the following nondimensional equation:

$$\mathrm{PFN} = \frac{kP^*}{\mu v w_0} \qquad (1)$$

PFN = prepreg flow number
k = fiber permeability (m^2)
v = linear speed of prepregging (m/s)
P^* = effective pressure depending on roller arrangement ($kg/m\ s^2$)
w_0 = final prepreg width (m)
μ = resin viscosity (Pa s)

Detailed derivation for the PFN may be found elsewhere.[11] The PFN can be interpreted as a ratio of the time required for the resin to penetrate from the top to the bottom of the fibers, over the time necessary to spread across the width of the prepreg. The optimum value of the prepreg number is unity. However, successful impregnation can occur over a wider range (i.e., PFN ≥ 1). It is simply less efficient as some resin is wasted. During impregnation, the width of the prepreg does not change significantly, while the permeability, k, remains constant. It can easily be seen that impregnation with viscous resin must be accompanied by slower impregnating speeds and/or increased roller pressure.

The NMP in solution B was evaporated until the resin content increased from 27 to 36%. It was desirable to have as high a resin content as possible, while still maintaining a desirable viscosity for impregnation. A good-quality prepreg was produced at a speed of 1.1 cm/s, approximately 0.1 MPa average pressure using two rollers, with the impregnation zone and the doctor plate heated to 100°C.[9] The prepreg was only slightly sticky as it went onto the take-up roller. The weight fraction resin in the prepreg was calculated to be 31.5% resin and the width of the prepreg increased from 2 to 3 cm, which indicated that good wetting was occurring.

Processing Cycles

A series of experiments were performed with each resin. The best results were obtained when the prepreg was dried as much as possible before stacking the plies and placing them in the press. The drying temperature was 150°C in a circulating oven. This temperature was sufficient to remove most of the NMP and it did not advance the polymer. In the press the laminate was wrapped with a semipermeable bleeder cloth, which allowed the residual solvent to escape. The laminates were heated in the press before pressure was applied. This has been found to enhance the mechanical properties of the composite.[12] By proper selection of processing cycles, well-consolidated laminates with very few voids were produced. A typical impregnating and drying se-

Table III Processing Effects on Resin and Solvent Contents for Prepreg Made with Sample B

Processing Step	Total Weight (g)	% Fibers	% Resin	% NMP
After impregnating	9.36	25	20	55
After drying	5.80	40	32	27
Final wt. [assumed (0% NMP)]	4.21	56 (50)[a]	44 (50)[a]	0

[a] Values in parentheses are in volume fraction, all others are in weight fraction. Volume fraction calculated using fiber density = 1.75 g/cm^3 and resin density = 1.38 g/cm^3.

quence for sample B is listed in Table III. Experiments with samples A and C used similar procedures.

The final weight fraction resin was calculated assuming there was no residual NMP in the laminate after processing. The resin content for the samples with the fewest voids was measured. Samples A, B, and C had resin contents of 18, 42, and 34%, respectively. In a TGA of the composite, a weight loss of only 1.4% up to 350°C was observed, which indicates that the assumption of no residual NMP in the final composites is reasonably accurate. TGA was also performed on the polymer powder of resin C. Using the following equation:

$$w_r = \frac{1 - w_{rc}}{1 - w_{rp}} \tag{2}$$

w_r = weight fraction resin in composite
w_{rc} = residual weight fraction composite
w_{rp} = residual weight fraction polymer

a weight fraction $w_r = 0.29$ was calculated.

Several laminates were processed and compared with the results found in the literature.[13-15] The best results were obtained when the prepreg was dried as much as possible before stacking the plies in the press. The minimum processing requirements were 1.38 MPa (200 psi), at 354°C for 5–15 min to ensure good consolidation. Insufficient drying of the prepreg results in excessive voids, especially at the ply interfaces.

Modeling

For both the prepregging and consolidation cycles, viscosity plays a major role in determining the specific time–temperature profiles. Accordingly, constitutive relations for predicting viscosity as a function of time, temperature, and concentration were developed for the PAI system. In addition, based on derived activation energies, a time–temperature equivalence model for determining a process cycle was also developed.

Viscosity Prediction

The viscosity data for resin C were plotted in Arrhenius form for both the temperature and concentration effects, as can be seen in Figure 6. For temperature dependence, the data points were fitted to the basic Arrhenius expression, viz.

$$\eta = \eta_0 e^{[E_a^T/RT]} \tag{3}$$

η, η_0 = viscosity, reference viscosity at concentration C and reference temperature T_0
E_a^T = activation energy for the temperature-dependent Arrhenius expression of viscosity
T = temperature
R = universal gas constant, 8.314 J/mol K^{-1}

For concentration dependence, the data points were also fitted to an exponential expression, viz.

$$\eta = \eta_0 e^{[k''c]} \tag{4}$$

η, η_0 = viscosity, reference viscosity at zero concentration and temperature T
k'' = proportionality constant
c = concentration of polymer, by weight fraction, in solution (dimensionless)

A linear relation was obtained by fitting Eqs. (3) and (4) for each data set. The values of the constants were averaged to give

$$k'' = 30.1$$

$$E_a^T = 32{,}700 \text{ J/mol}$$

Substituting the constants and solving Eq. (4) for

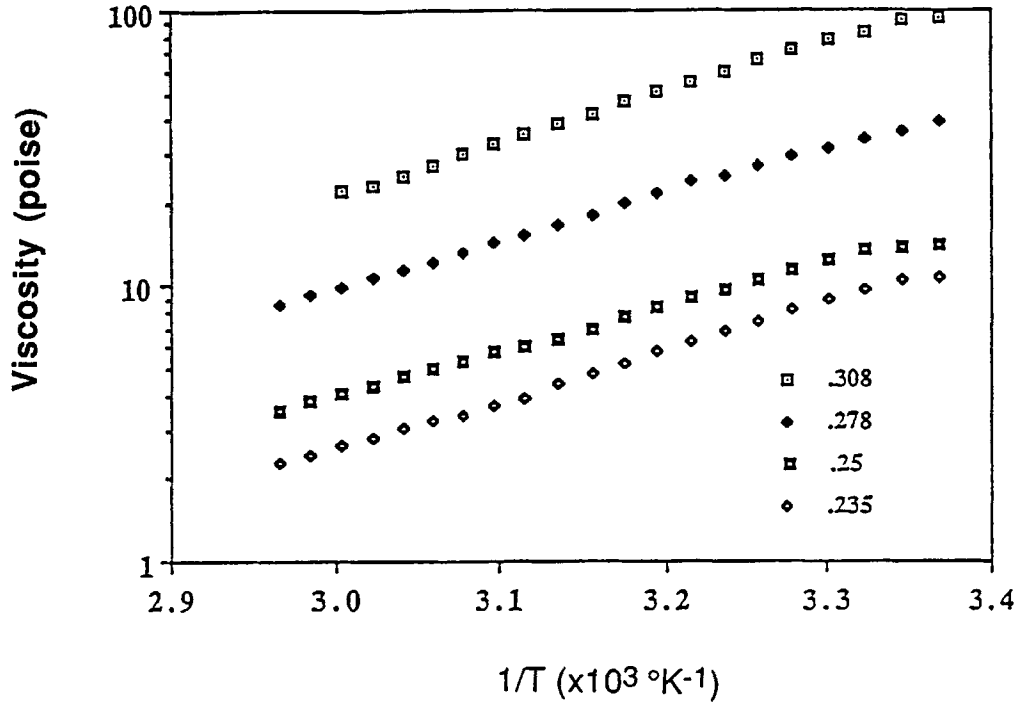

Figure 6 Arrhenius plot of sample C (M_w 24,600) viscosity for different polymer concentrations (by weight). $1/T$ ($\times 10^3$ K^{-1}). Inverse temperature in $\times 10^{-3}$ K^{-1} units.

zero concentration, a value $\eta_0 = 10^{-2.338}$ is obtained, which is essentially 1 cP, the value expected for pure NMP.

The two equations were combined to give the following expression:

$$\eta = \eta_0 \exp\left(\frac{E_a^T}{RT} + \frac{E_a^c}{RT_r} C\right) \tag{5}$$

where the concentration constant k'' has been expressed as an activation energy defined by

$$k'' = \frac{E_a^c}{RT_r} \tag{6}$$

with

E_a^c = 74,600 J/mol, activation energy for the concentration-dependent Arrhenius expression of viscosity
T_r = reference temperature, taken as room temperature 298 K

It can easily be seen from the preceding equation that the concentration may be expected to have a pronounced effect on viscosity. The TGA data and the predicted viscosity for a 6°C/s ramp are shown in Figure 7. This expression for viscosity is quite useful since the viscometer is not capable of accurately measuring the viscosity once evaporation starts. In the viscometer, the solution quickly turns from being a thin solution to a solid film. The figure shows the viscosity is initially controlled by the temperature, but it is quickly dominated by the concentration once evaporation begins.

Time–Temperature Superposition

Time–temperature superposition has been used extensively in viscoelastic processes to predict long-term effects from short-term experiments.[16] The same approach can be applied to kinetic processes using an Arrhenius equation to relate time and temperature.[17,18] The equation can be expressed as

$$t = t_r \exp\left[\frac{E_a^s(T_r - T)}{RTT_r}\right] \tag{7}$$

t, t_r = time, reference time (s)
T, T_r = temperature, reference temperature (K)
E_a^s = activation energy (J/mol) of the superposition
R = gas constant (J/mol K^{-1})

The time–temperature superposition method is useful in estimating the activation energy of kinetic processes, which are not easily studied by conven-

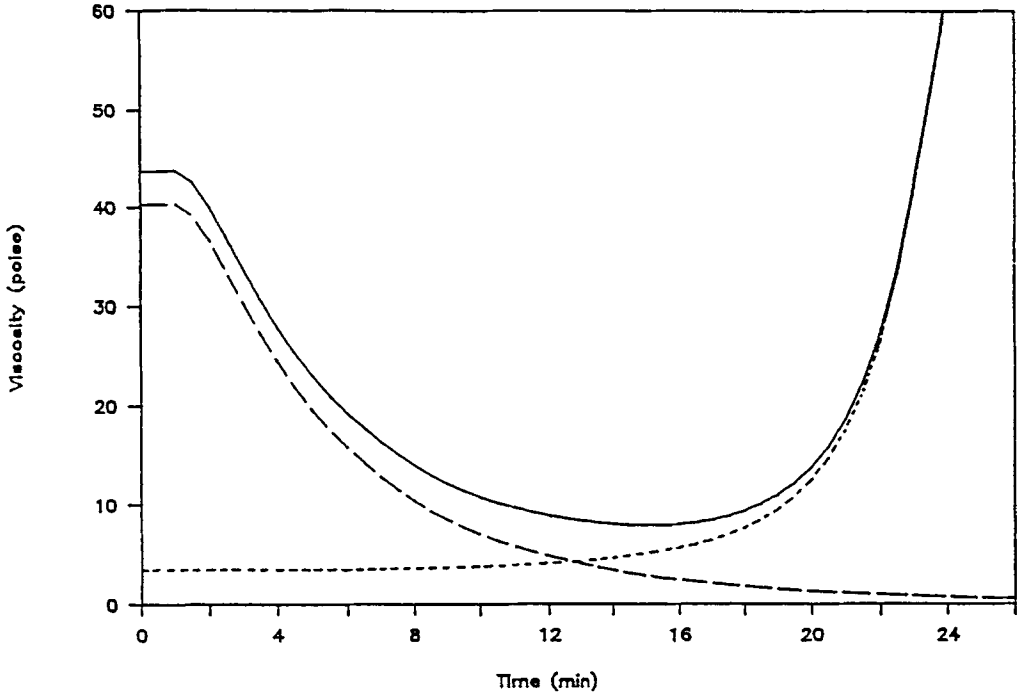

Figure 7 Predicted viscosity as a function of time shown as the the sum of the temperature and concentration functions. Concentration: – • – • – • – • –; temperature: - - - - -; sum: ——.

tional techniques. Time–temperature superposition is used to calculate a kinetic pathway from one thermodynamic state to another, when referenced to an event with the same initial and final states. The principle of time–temperature can be applied to any kinetic process with constant activation energy. It can be used to predict degree of cure, weight loss, viscosity, etc. The activation energy, which relates time and temperature, can be obtained from the shift factor required to superimpose a series of isothermal data.

For example, Eq. (7) can be used to predict the effects of an evaporation process. An isothermal weight loss experiment is performed to generate a reference set of data. Using this data and the activation energy for the process, the time required for evaporation can be estimated at different temperatures. The equation can also be used to express the effects of any isothermal hold in terms of a reference experiment at a given temperature. The time required for evaporation at a higher temperature is shorter, but it has the same effect as a longer hold, t_r, at the lower temperature. The effect of an isothermal hold at a higher or lower temperature can be expressed as equivalent isothermal time (EIT) in terms of the reference experiment.

Integration of Eq. (7) allows nonisothermal temperature profiles to be referenced to an equivalent isothermal time. The t_r and T_r are determined from the nonisothermal temperature profile:

$$\text{EIT} = t = \int_0^{t_r} \exp\left[\frac{E_a(T_r - T)_{t_r}}{R(TT_r)_{t_r}}\right] dt_r' \qquad (8)$$

The calculation of time for a nonisothermal hold is the summation of small isothermal segments of time dt_r, (or Δt_r), while the T_r is changing. This allows the effect of a nonisothermal temperature profile to be expressed in terms of an isothermal experiment. The EIT is specific to the temperature at which the experiment was performed.[17,18]

The experimental data does not necessarily need to be generated from an isothermal experiment. A temperature profile can be expressed in terms of a dynamic experiment, or equivalent dynamic time (EDT). This can still be viewed as the summation of isothermal events, but for this case, both T and T_r are changing in Eq. (8).

The principle of time–temperature superposition was applied to the evaporation of NMP solvent from the PAI solutions. Four different isothermal temperatures were used to evaporate the NMP from solution C in the TGA. The activation energy was obtained by measuring the time required for the evaporation to reach a chosen point at two different temperatures. An average value of 22,000 J/mol was used for the EIT calculations.

Application of the Time–Temperature Superposition

The weight loss curve at 142°C was chosen to be the reference experimental curve. Equation (7) was used to predict the effects of solvent evaporation at different temperatures. Figure 8 shows the reference data at 142°C, the predicted weight loss curve at 108°C, and the actual data at 108°C. It can be seen that the predicted curve will have the same initial and final states as the experimental data. The final weight loss for the experiments at 142°C and 108°C were close to the same value. Figure 9 shows three hypothetical temperature profiles as a function of time. One is an isothermal hold at 142°C, one is a 1°C/min ramp to 167°C, and the other is a continuous 0.665°C/min ramp over the 300-min time scale. Equation (8) was used to convert the temperature profiles to an EIT at 142°C. Figure 10 shows the relationship of EIT at 142°C to real time. Since the 142°C profile is equal to the reference 142°C, the EIT is equal to the real time. The other two temperature profiles are initially at lower temperatures than the reference, and their time is "worth" less than time spent at 142°C; EIT is less than real time. As the temperature passes 142°C, it becomes worth more than time spent at 142°C, and EIT increases faster than the real time. At 300 mins the three temperature profiles have the same effect. This curve can be used in conjunction with the isothermal weight loss curve, shown in Figure 8, to predict the weight loss at a specific time and establish an equivalent weight loss for the different temperature profiles.

The time–temperature superposition can also be used to predict the viscosity described by Eq. (5). The same activation energy can be used for viscosity as the one used for the weight loss curve because the temperature effect on viscosity becomes negligible compared with the concentration effect. The isothermal hold at 142°C evaporated the solvent too quickly to observe a decrease in viscosity, so it was not the desired reference for the prediction of viscosity. The lowering of viscosity with temperature, before the concentration dominates the viscosity, was not observed with any of the four isothermal holds, but it can be seen using a 6°C/min temperature ramp, as shown in Figure 11. This can be used as the reference experiment for the EDT. Figure 12 shows the EDT at a 6°C/min ramp, as compared with real time. The 6°C/min ramp is plotted as a reference, compared with a 150°C isothermal hold and a 12°C/min ramp to 150°C.

Equivalent dynamic time can be used to estimate the time and temperature where the viscosity begins to increase. Figure 11 shows that the viscosity is

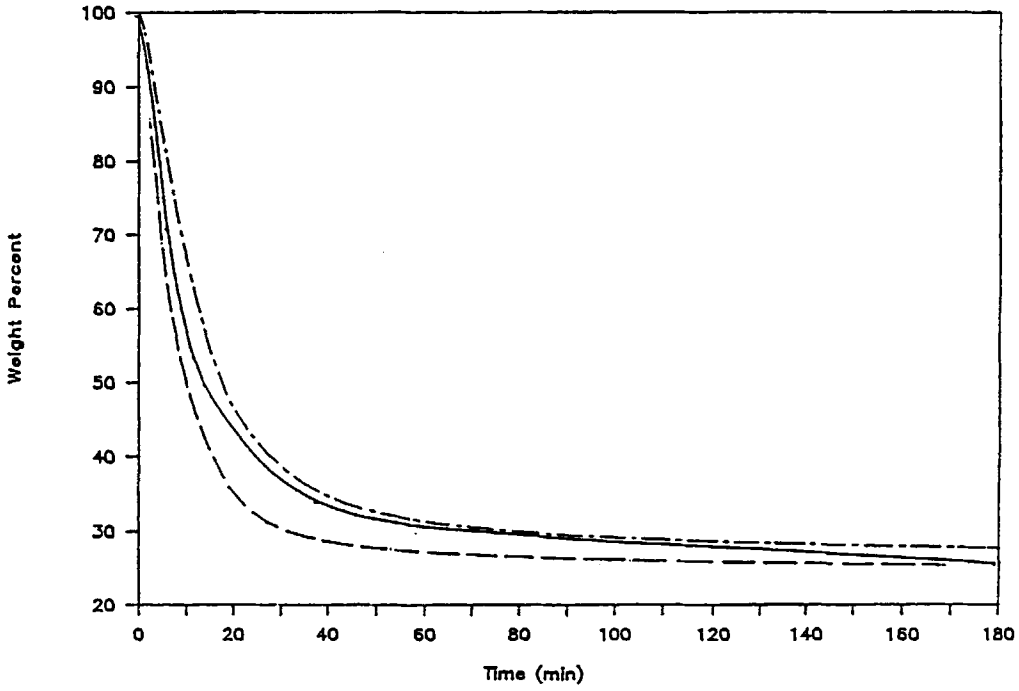

Figure 8 Predicted 108°C isothermal weight calculated from 142°C isothermal data using equivalent isothermal times (EIT). Curves are keyed as follows: Data at 108°C -·-·-·-·-; isothermal data at 142°C ------; predicted from EIT at 108°C ——.

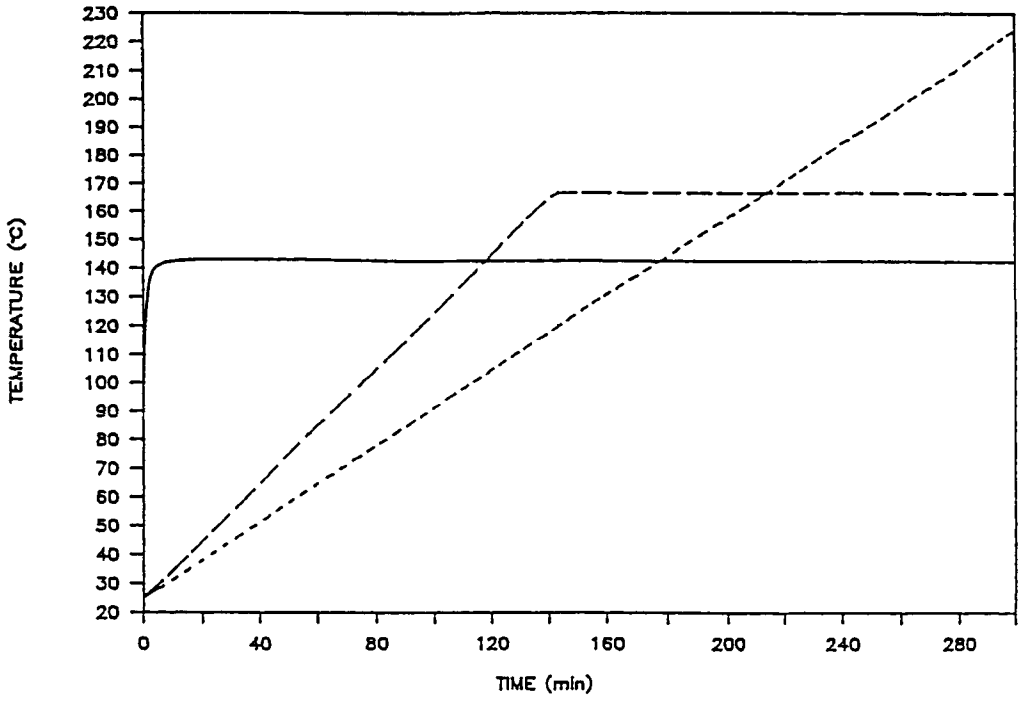

Figure 9 Three actual temperature profiles used to calculate equivalent isothermal times (ELT): Isothermal 142°C ——; dynamic 1°C/min. - - - - for 120 min followed by 170°C isothermal hold; dynamic 0.665°C/min. ----------.

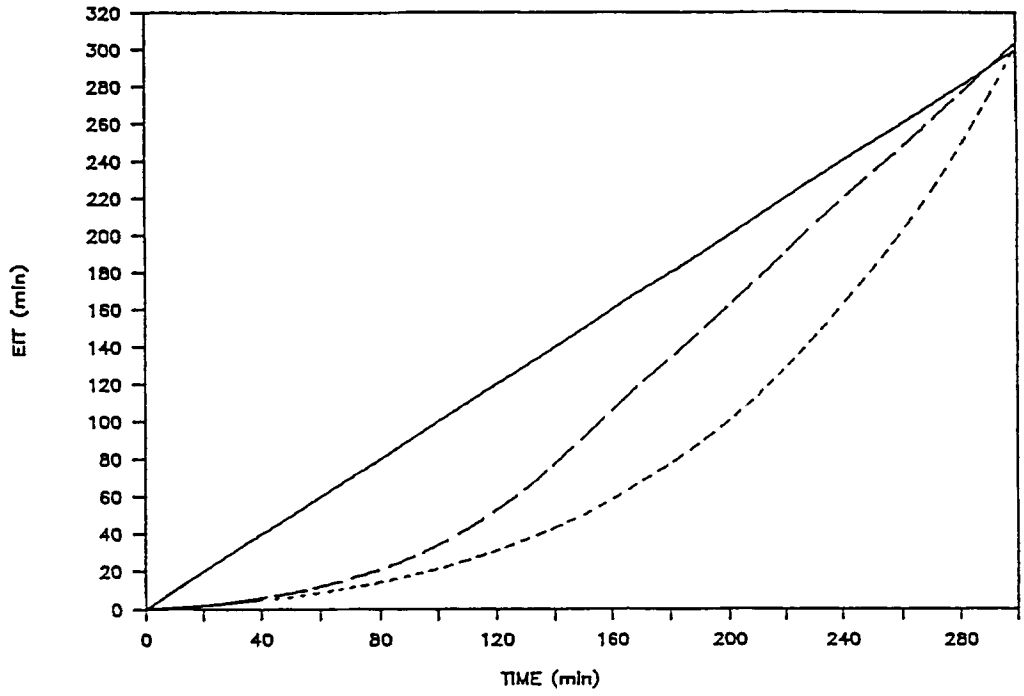

Figure 10 The equivalent isothermal times for the temperature profiles of Figure 9 using 142°C isotherm as the reference: Reference 142°C ——; dynamic 1°C/min. - - - - followed by 170°C isothermal hold; dynamic 0.665°C/min. ----------.

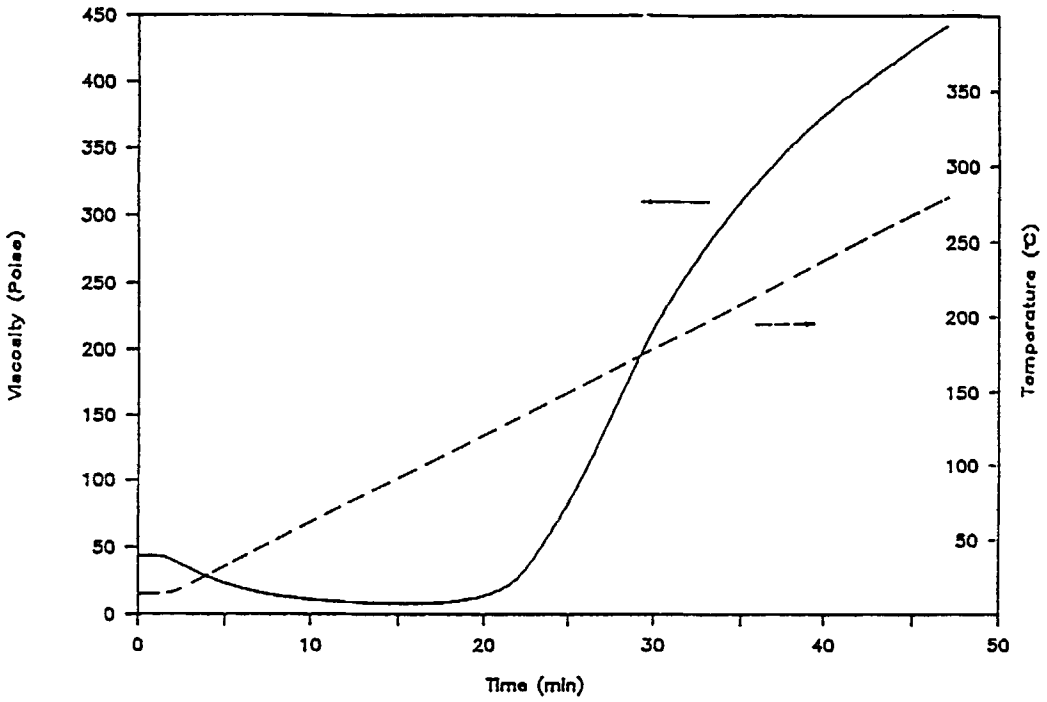

Figure 11 Predicted viscosity as a function of time for sample C (M_w 24,600) using Eq. (5).

approximately 100 P at 25 min for a 6°C/min ramp. To estimate the time that the 12°C/min ramp reaches 100 P, the EDT value of 25 min is read from the y axis of Figure 12 over to the point where it intersects the curve, and down to the x axis to determine real time. The EDT of 25 min is equal to approximately 9 min real time for the 12°C/min ramp, which occurs at 108°C. The same procedure can be performed with the 150°C isothermal hold or any other temperature profile.

Collectively, this information was used in establishing reproducible processing cycles for the different PAI resin systems examined.

CONCLUSIONS

Commercially available PAIs, primarily used as adhesives and fiber solution, show promise for use as matrices in high-performance carbon fiber composites. Their high glass transition temperature and mechanical properties put them in an elite class of materials. Unfortunately, the processing of these materials requires additional measures to accommodate the evolution of solvents and the subsequent crosslinking. It is because of these special processing measures or requirements that this investigation was performed.

Thermal analysis of three poly(amide imide) NMP solutions, each differing by molecular weight, was used for characterization. The solutions varied slightly in concentration from 73% NMP by weight for the two lower molecular weight polymers to 78% for the 24,600 molecular weight solution. Degradation of the polymer began at 500°C after the solvent had been driven off. The glass transition of the polymer was 291, 304, and 329°C, identified by the maximum of tan δ using dynamic mechanical analysis.

A good-quality, unidirectional prepreg was produced on a small-scale prepreg machine. The best results were achieved by drying the prepreg prior to stacking and consolidation. Good composites as evaluated by optical microscopy were produced with a minimum of 1.38 MPa (200 psi) and 354°C from 5 to 15 min. Impregnation of the carbon fiber tows was found to be strongly dependent on the viscosity of the polymer solutions used, and the prepreg flow number (PFN) was utilized to establish appropriate impregnation conditions. The viscosity of the solution was modeled using an Andrade expression for an activated complex with two independent variables, polymer concentration C, and temperature T. The viscosities of the polymer solutions were sensitive to small changes in solvent concentrations, such as that which would occur during a typical isothermal prepregging run. An application of the

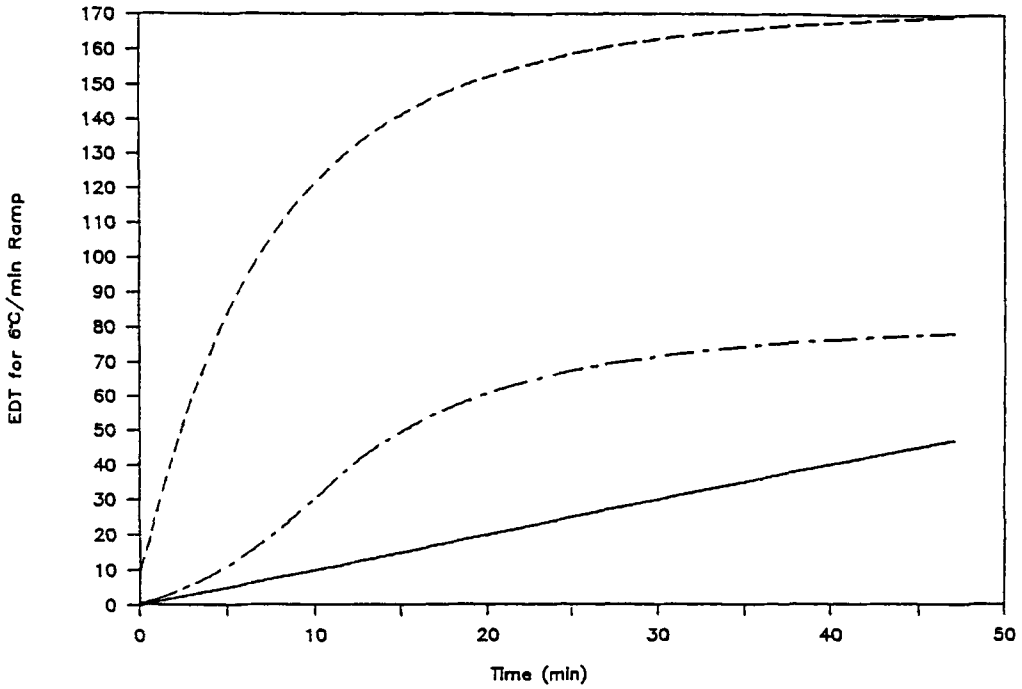

Figure 12 Equivalent dynamic time (EDT) for a 6°C/min ramp as a function of time: Reference 6°C/min. ——; isothermal 150°C ------; dynamic 12°C/min followed by isothermal hold at 150°C - • - • - • -.

equivalent isothermal time concept described the loss of solvent in the system by time transformation to a single isothermal weight loss curve. This description was successfully applied to predict the weight loss for a 108°C isotherm from 142°C isothermal data. The concept of the time–temperature superposition and the modeling of viscosity was found useful in understanding the rheological behavior of PAI solutions in both prepregging and consolidation processes.

The authors acknowledge Dr. Karl Nelson and Dr. Kyujong Ahn of the Polymeric Composites Laboratory for helpful discussions and coordination with this project. Financial assistance provided by Rhone Poulenc through project support to the Polymeric Composites Laboratory at the University of Washington is gratefully acknowledged.

REFERENCES

1. E. F. Oleinik, *Polym. J.*, **19**(1), 105 (1987).
2. R. H. Walker, *Soc. Plast. Eng. Tech. Pap.*, **20**, 92 (1974).
3. N. Tsubokawa, M. Sakaguchi, and Y. Sone, *Kobunshi Ronbunshu*, **45**(3), 263 (1988).
4. N. Tsubokawa, I. Yamamoto, and Y. Sone, *Konbunshi Ronbunshu*, **44**(11), 831 (1988).
5. C. J. Billerbeck and S. J. Henke, *Engineering Thermoplastic Properties and Applications*, J. Margolis, Ed., Marcel Dekker, New York, 1985, p. 373.
6. G. H. Hardesty, *Soc. Auto. Eng., SP-597* (Aerospace Cong./Exp.), (1984).
7. N. J. Johnston and P. M. Hergenrother, *32nd Int. SAMPE Symp.*, 1400, (1987).
8. B. W. Cole and W. C. Crowe, *Proc. Soc. Plast. Eng./APC '88*, 207 (1988).
9. W. J. Lee, J. C. Seferis, and D. C. Bonner, *SAMPE Q*, **17**(2), 58 (1986).
10. J. F. Dezern, *SAMPE J.*, Mar./Apr., 27 (1988).
11. J. C. Seferis and K. Ahn, *Proc. 34th Int. SAMPE Symp.*, **34**, 63 (1989).
12. D. F. Hiscock and D. M. Bigg, *Polym. Comp.*, **10**(3), (1989).
13. B. W. Cole and G. T. Brooks, Amoco, U.S. Pat. 4,579,773.
14. Toray Indus., Japanese Patent, 59,202,819, [84,202,819].
15. B. Cole, *Proc. 30th Int. SAMPE Symp.*, **30**, 799 (1985).
16. Z. Tadmor and C. G. Gogos, *Principles of Polymer Processing*, Wiley, New York, 1979.
17. R. B. Prime, *Proc. 14th NATAS Conf.*, 137, 1985.
18. R. B. Prime and C. H. Moy, *SPE ANTEC '88 Conf. Proc.*, **47**, 1099 (1989).

Received January 21, 1991
Accepted February 11, 1991